Purification and Structural Characterization of Transforming Growth Factor Beta Induced Protein (TGFBIp) from Porcine and Human Corneas†

Rolf B. Andersen,‡ Henrik Karring,‡ Torben Møller-Pedersen,§ Zuzana Valnickova,‡ Ida B. Thøgersen,‡ Chris J. Hedegaard,‡ Torsten Kristensen,‡ Gordon K. Klintworth,|| and Jan J. Enghild*,‡

Department of Molecular Biology, University of Aarhus, Gustav Wieds Vej 10C, DK 8000 Aarhus C, Denmark, Department of Ophthalmology, Aarhus University Hospital, Nørrebrogade 44, DK 8000 Aarhus C, Denmark, and Departments of Pathology and Ophthalmology, Duke University Medical Center, Durham, North Carolina 27710

Received July 4, 2004; Revised Manuscript Received October 11, 2004

ABSTRACT: Mutations in the *TGFBI* (*BIGH3*) gene that encodes for transforming growth factor beta induced protein (TGFBIp) are the cause of several phenotypically different corneal dystrophies. While the genetics of these protein misfolding diseases are well documented, relatively little is known about this extracellular matrix protein itself. In this study, we have purified TGFBIp from normal human and porcine corneas using nondenaturing conditions and standard chromatography techniques. The two homologues were shown to be monomers, and we did not find evidence for posttranslational additions. The C-terminal of both human and porcine TGFBIp is truncated predominantly after the integrin binding sequence Arg_{642}−Gly_{643}−Asp_{644} (RGD). However, using an antibody against the C-terminal fragment (residues 648−683), we also detected a small amount of full-length TGFBIp in corneal extracts. Approximately 60% of TGFBIp was covalently associated with insoluble components of the extracellular matrix in both human and porcine corneas through a disulfide bridge.

The *TGFBI*[1] gene, also known as *BIGH3*, was discovered in a search for genes induced by transforming growth factor β (TGF-β) (*1*). On the basis of the cDNA sequence, it is predicted to encode for a 72 kDa protein composed of 683 amino acid residues including a signal peptide (*1*).

The physiological function of transforming growth factor beta induced protein (TGFBIp) has not yet been characterized, but it is a highly conserved protein dominated by four fasciclin (FAS) domains in close succession. The protein homologues from human and porcine are 93% identical (Figure 2). FAS-containing proteins are extracellular or membrane bound and associated with cell adhesion. Whereas TGFBIp itself appears to be restricted to vertebrates, the FAS domain has been identified within Eukarya in Plantae, Fungi, and Animalia (*2*−*7*). However, only four proteins containing the domain are known in humans, including TGFBIp, periostin (*8*, *9*), and two newly described proteins, FEEL-1 and FEEL-2 (*10*−*12*). FAS domains are recognized more from their overall homology than any particular consensus sequence, but three moderately conserved areas denoted Fra, H-box, and Frb are usually present (*13*). FAS domains are often present in multiple copies in the same protein and displaying low internal sequence identity reflecting an ancient multiplication event. The structure of FAS domains from two different proteins has recently been solved (*7*, *14*), and shown to be a unique domain fold consisting of a seven-stranded β-wedge and a number of α-helices. The structure has made it possible to model part of TGFBIp, which has provided insight into the mutation sites responsible for corneal mutations and possible ligand binding areas (*15*). However, there is no immediate clue to the adhesion mechanism of FAS domains.

TGFBIp is found in the extracellular matrix (ECM) of most tissues. Cornea (*16*, *17*), skin (*18*), bone (*19*), tendon (*20*, *21*), endometrium (*22*), and kidney (*23*) all have high levels of TGFBIp. During embryogenesis, *TGFBI* is expressed in mesenchyme and mesenchymal-derived tissues, particularly in active zones of growth (*24*, *25*). Most cell lines studied express TGFBIp at low levels unless induced by TGF-β. An exception is the fibroblast, which produces TGFBIp constitutively at significant levels (*18*). The most telling pattern of distribution for TGFBIp is probably the extensive co-localization with bovine collagen VI (*26*), which has been emphasized by the recent finding that TGFBIp may bind to bovine collagen VI through a disulfide bond (*27*).

† The work was supported by National Eye Institute Grant R01 EY 12712, the Danish Association for Prevention of Eye Diseases and Blindness, the Synoptik Foundation, Aarhus University Research Foundation, and the Danish Medical Research Council.

* To whom correspondence should be addressed: Department of Molecular Biology, University of Aarhus, Gustav Wieds Vej 10, 8000 Aarhus C, Denmark. Phone: +45 8942 5062. Fax: +45 8942 5063. E-mail: jje@mb.au.dk.

‡ Department of Molecular Biology, University of Aarhus.

§ Department of Ophthalmology, Aarhus University Hospital.

|| Duke University Medical Center.

[1] Abbreviations: *TGFBI*, transforming growth factor beta induced gene; *BIGH3*, TGF-β induced human gene 3; TGF-β, transforming growth factor β; TGFBIp, transforming growth factor beta induced protein; FAS, fasciclin; ECM, extracellular matrix; HFBA, heptafluorobutyric acid; ECL, enhanced chemiluminescence; SDS, sodium dodecyl sulfate; PAGE, polyacrylamide gel electrophoresis; MALDI-TOF, matrix-assisted laser-desorption ionization time-of-flight; MS, mass spectrometry; ESI, electrospray ionization; LC-MS/MS, liquid chromatography tandem mass spectroscopy; MS/MS, tandem mass spectroscopy; rhTGFBIp, recombinant human TGFBIp; IgG, immunoglobulin G.

10.1021/bi048589s CCC: $27.50
Published on Web 11/26/2004

In addition to bovine collagen VI, TGFBIp has been shown to interact with porcine collagens I, II, and IV (*28*), human fibronectin (*29*), and human integrins α3β1 (*30*, *31*), α1β1 (*32*), αvβ5 (*33*), and α6β4 (*34*). The interaction of TGFBIp with these ligands suggests that TGFBIp plays a role in cell adhesion. In the case of some integrins, TGFBIp may bind through the RGD sequence situated near the C-terminus of TGFBIp (Figure 2).

Several corneal dystrophies in humans are accompanied by mutations in *TGFBI* (*35*, *36*) causing an abnormal accumulation of protein aggregates in the cornea (*36*). While symptoms are restricted to the cornea, the resulting reduction in visual acuity may progress to severe visual impairment. The protein deposits in *TGFBI*-linked corneal dystrophies have been shown to bind antibodies against TGFBIp (*37*, *38*), indicating that they consist, at least partly, of TGFBIp. Some *TGFBI* mutations give rise to a deposition of amyloid within the corneal stroma (R124C, L518P, L527R, A546D, A546T, P501T, A622H, and H626R), while others cause fuchsinophilic granular deposits (R124L, R124S, R555W, and G623N), a combination of granular and amyloid deposits (R124H), or curly fibers (R555Q) (*36*, *39*). This tight linkage between specific mutations and particular kinds of protein aggregation is unique to the *TGFBI*-linked corneal dystrophies, and may help elucidate the requirements for the formation of amyloid deposits in general.

Little biochemical information regarding the fundamental characteristics of TGFBIp has been available until now, largely because TGFBIp has not been purified in its native state. This study reports the purification and structural characterization of TGFBIp from porcine and human corneas. Both homologues were shown to be monomers lacking posttranslational additions. The majority of TGFBIp in the cornea was C-terminal truncated after the RGD sequence. However, the results indicate that the C-terminal proteolytic processing of corneal TGFBIp is a heterogeneous event leading to a ragged C-terminus. In addition, a fraction of TGFBIp was covalently associated with insoluble extracellular components.

EXPERIMENTAL PROCEDURES

Materials. Unless otherwise noted chemicals were from Sigma Chemical Co., St. Louis, MO. HPLC-grade acetonitrile was from Mallinckrodt Baker (Mallinckrodt Baker, Deventer, Holland). Heptafluorobutyric acid (HFBA) was purchased from Pierce (Rockford, IL). Sequence grade porcine trypsin was from Promega (Madison, WI). Protein sequencing and peptide synthesis reagents were from Applied Biosystems (Foster City, CA). Prepacked columns, chromatography resins, and ECL Western blotting detection reagents were from Amersham Biosciences (Little Chalfont, England). SDS−PAGE molecular weight standards were purchased from Bio-Rad Laboratories (Hercules, CA). Fused-silica emitters and boro-silicate spray capillaries for on-line nanoelectrospray were obtained from Proxeon Biosystems (Odense, Denmark) and New Objective (Woburn, MA). Reverse phase column material (Nucleosil 120−3 C_{18}) was from Macherey-Nagel (Duren, Germany).

Human and Porcine Corneas. Thirteen normal human corneas were obtained post mortem from individuals intended for autopsy at the Department of Forensic Medicine, Aarhus University Hospital, Denmark. None of the individuals had any known corneal disease or previous eye surgery. The corneas came from 47−87-year-old individuals and the interval from death to preparation of the cornea ranged from 19 to 56 h. Following informed consent, one additional cornea was obtained from a 53-year old man immediately after enucleation for a uveal melanoma. The collection of human tissue was approved by the regional committee for scientific medical ethics in Aarhus, Denmark. Porcine eyes were obtained freshly from Danish Crown (Horsens, Denmark). The central area of both human and porcine corneas was excised using a 7-mm diameter trephine. The corneas were kept at −20 °C until use.

Purification of TGFBIp from Porcine and Human Corneas. The corneas were placed in a vacuum desiccator for 24−48 h, and the dried corneas were homogenized in liquid nitrogen using a tissue homogenizer (Ystral, Ballrechten-Dottingen, Germany). The resulting corneal powder was washed three times for 5 min in 75 mL of cold 20 mM Tris-HCl, pH 7.4, and centrifuged for 10 min at 30000*g* in between. Following the last centrifugation step, the pellet was left stirring overnight at 4 °C in extraction buffer (1 M $(NH_4)_2SO_4$, 20 mM Tris-HCl, pH 7.4). The resulting extract was passed through a 0.45 μm filter, and applied to a 5 mL Phenyl Superose FF Hi-Trap column (Amersham Bioscience) equilibrated in the extraction buffer. Bound proteins were eluted by employing a linear gradient from 1 to 0 M $(NH_4)_2SO_4$. The flow rate was 0.5 mL/min, and the eluate was monitored at 280 nm. The TGFBIp-containing fractions were pooled and applied to a 3 mL Protein G column (Amersham Bioscience) equilibrated in 20 mM Tris-HCl, pH 7.4. The flow-through was dialyzed against 20 mM Tris-HCl, pH 7.4 at 4 °C for 12−16 h. The dialyzate was applied to a 1 mL Mono Q High-Trap anion exchange column (Amersham Bioscience) equilibrated in 20 mM Tris-HCl, pH 7.4, and the proteins were separated using a linear gradient from 0 to 1 M NaCl in 20 mM Tris-HCl, pH 7.4 at a flow rate of 1 mL/min. TGFBIp eluting from 0.5 to 0 M $(NH_4)_2SO_4$ was pooled, concentrated, and applied to a Superose 12 HR 10/30 gel filtration column (Amersham Bioscience) equilibrated in 50 mM Hepes, pH 7.4, 150 mM NaCl, 0.02% NaN_3. The column was run in the same buffer with a flow rate of 0.3 mL/min. The purified TGFBIp was frozen at −20 °C. All chromatographic steps were performed at room temperature (∼20 °C) using a Pharmacia FPLC system. The purification was monitored using Western blotting, and the intensity of the signals was quantified in a Kodak Image Station 1000 equipped with a cooled CCD camera using proprietary software.

Expression and Purification of Recombinant Human TGFBIp (rhTGFBIp). The human *TGFBI* (*BIGH3)* cDNA clone (Invitrogen) was obtained from a human placenta cDNA library cloned in the pCMV−SPORT6 vector. Expression was performed in HEK293 cells transfected using the calcium phosphate precipitation method. Cells were grown in serum-free DMEM medium supplemented with glutamine and the secretion of TGFBIp was followed by immunoblotting. Media were harvested and recombinant TGFBIp was basically purified as described for corneal TGFBIp.

Amino Acid Sequence Analysis. N-terminal sequence analysis was performed in an Applied Biosystems 477A

sequencer with on-line phenylthiohydantoin analysis using an Applied Biosystems 120A HPLC system operated according to the manufacturer's recommendations. C-terminal sequence analysis was carried out by Protein Analysis Center, Karolinska Institutet, Stockholm, Sweden using an Applied Biosystems Procise C instrument as described by Bergman et al. (*40*).

Matrix-Assisted Laser Desorption Ionization Time-of-Flight (MALDI-TOF) Mass Spectrometry. For MALDI-TOF peptide fingerprinting a Micromass Q-TOF Ultima Global mass spectrometer was used. The samples were mixed with α-cyano-4-hydroxy-cinnamic acid at 2 mg/mL in 50% AcCN/0.3% TFA to the desired concentration and 0.5 μL was spotted on a MALDI target for analysis. The masses of purified porcine and recombinant human TGFBIp were determined under nonreducing conditions using a Voyager-DE STR mass spectrometer operated in linear mode using sinapinic acid as matrix.

Electrospray Ionization (ESI) Mass Spectrometry. Porcine or human corneal powders were boiled in reducing SDS sample buffer and analyzed by reduced SDS−PAGE. The TGFBIp bands of interest were excised and digested with different proteases overnight, the peptides were extracted, and particular matter was removed by filtration. The LC-MS/MS analyses were performed using a Micromass Q-TOF Ultima Global mass spectrometer connected to an LC−Packings UltiMate Nano LC system with autosampler. A nano spray ion source was used to hold the packed fused-silica emitters and apply capillary voltage through a Valco union. Injected samples were first trapped and desalted isocratically on an LC−Packings PepMap C18 Precolumn cartridge (300 × 5 mm). The peptides were eluted and separated on analytical fused-silica emitter (10 cm × 75 mm, packed with Nucleosil 120−3, C18, Macherey-Nagel) connected in line to the mass spectrometer. The column was developed using a 200 nL/min flow rate and linear gradients from buffer A (0.02% HFBA and 0.5% acetic acid in water) to buffer B (0.02% HFBA, 0.5% acetic acid, and 75% acetonitrile in water). After data acquisition, the individual MS/MS spectra acquired for each precursor were combined, smoothed, deisotoped, and compiled as a single Mascot-searchable peak list. The peak list files were used to query the Swiss-Prot database using the Mascot program. Unmatched spectra were analyzed using the Mascot error tolerant search option (*41*).

Calibrated Gel Filtration. The apparent molecular mass and Stokes radii (R_s) of purified porcine TGFBIp were measured by gel filtration on a calibrated PC 3.2/30 Superose 12 column (Amersham Biosciences). The column was connected to a Pharmacia SMART system equilibrated in 50 mM Tris-HCl, pH 7.4, 150 mM NaCl, and calibrated using ∼20 μg of each of the following standard globular proteins with known molecular mass and Stokes radius: ribonuclease A (MW = 14.8 kDa, R_s = 16.4 Å), chymotrypsinogen A (MW = 21.0 kDa, R_s = 20.9 Å), ovalbumin (MW = 43.5 kDa, R_s = 30.5 Å), and bovine serum albumin (MW = 66.0 kDa, R_s = 35.5 Å). The elution volume (V_e) of the standard proteins was measured and K_{av} was calculated according to the equation: $K_{av} = (V_e - V_0)/(V_t - V_0)$. The elution position of blue dextran was used as the Superose 12 void volume (V_0 = 0.85 mL) and the total volume of the column (V_t) was 2.4 mL. The data were used for plotting K_{av} against log(MW) and $(-\log K_{av})^{1/2}$ against the Stokes radius (R_s) according to Siegel and Monty (*42*). The V_e of purified porcine TGFBIp was measured using 6 μg of protein. Eluting proteins were monitored at 280 nm. The V_e of purified human TGFBIp was monitored by immunoblotting of fractions.

Production of TGFBIp Fragments and Specific Antiserum. Human TGFBIp fragments for antibody production were either synthesized (residues 648−683; C-terminal) or expressed in *E. coli* (residues 134−500; central domains). The peptide corresponding to residues 648−683 in human TGFBIp was assembled in an Applied Biosystems 433A Peptide synthesizer using F-moc chemistry (*43*). The resulting peptide was deblocked, purified by reversed phased HPLC, and characterized by Edman degradation and mass spectrometry. Primers for amplifying the TGFBIp cDNA encoding residues 134−500 were 5′-caccgggcccggcagcttcaccatcttcg-3′ and 5′-tcaggggtcagcacccggtccat-3′. The resulting TGFBIp cDNA fragment was cloned into pET Directional TOPO expression plasmid (pET100/D-TOPO, Invitrogen), and transfected into *E. coli* cells. The TGFBIp fragment was purified using nickel affinity chromatography. Rabbits were immunized five times subcutaneously with approximately 100 μg of antigen emulsified in Freund's adjuvant at four week intervals.

Polyacrylamide Gel Electrophoresis and Western Blots. SDS−PAGE was performed in 5−15% gradient gels (10 cm × 10 cm × 1.5 mm) using the glycine/2-amino-2-methyl-1,3-propanediol/HCl system described by Bury (*44*). For Western blotting, proteins were electroblotted onto a PVDF membrane according to Matsudaira (*45*), and TGFBIp was detected with an enhanced chemiluminesence detection system (Amersham Biosciences) using the primary antisera at a dilution of 1:2000.

Quantification of Covalent-Associated TGFBIp. Approximately 1 mg of human corneal powder was incubated for 30 min at 25 °C in 100 μL of nonreducing SDS sample buffer containing 50 mM iodoacetamide interrupted by vigorous vortex mixing. The sample was then boiled for 5 min and centrifuged for 2 min at 16000*g* before the supernatant was removed and transferred to another Eppendorf tube. This procedure was repeated with the pellet four more times using nonreducing SDS sample buffer without iodoacetamide. The supernatants were combined producing a total volume of 0.5 mL. After the fifth time no TGFBIp was detected in the supernatant as determined by Western blotting. The resulting pellet was then boiled in 100 μL of SDS sample buffer now containing 50 mM DTT, centrifuged for 2 min at 16000*g* and the supernatant was transferred to another Eppendorf tube. The combined nonreduced supernatants and the protein material released following reduction of the pellet (1/10 of both) were analyzed by reduced SDS−PAGE (Figure 6). Proteins were electroblotted onto a PVDF membrane and TGFBIp was detected by immunoblotting using the primary antisera against the central domains of TGFBIp. Quantifications of TGFBIp were performed by densitometry on the developed films using a proprietary Software package (Biorad Quantity One).

RESULTS

Purification of Porcine and Human TGFBIp. To make the porcine corneas amenable to homogenization, they were dried

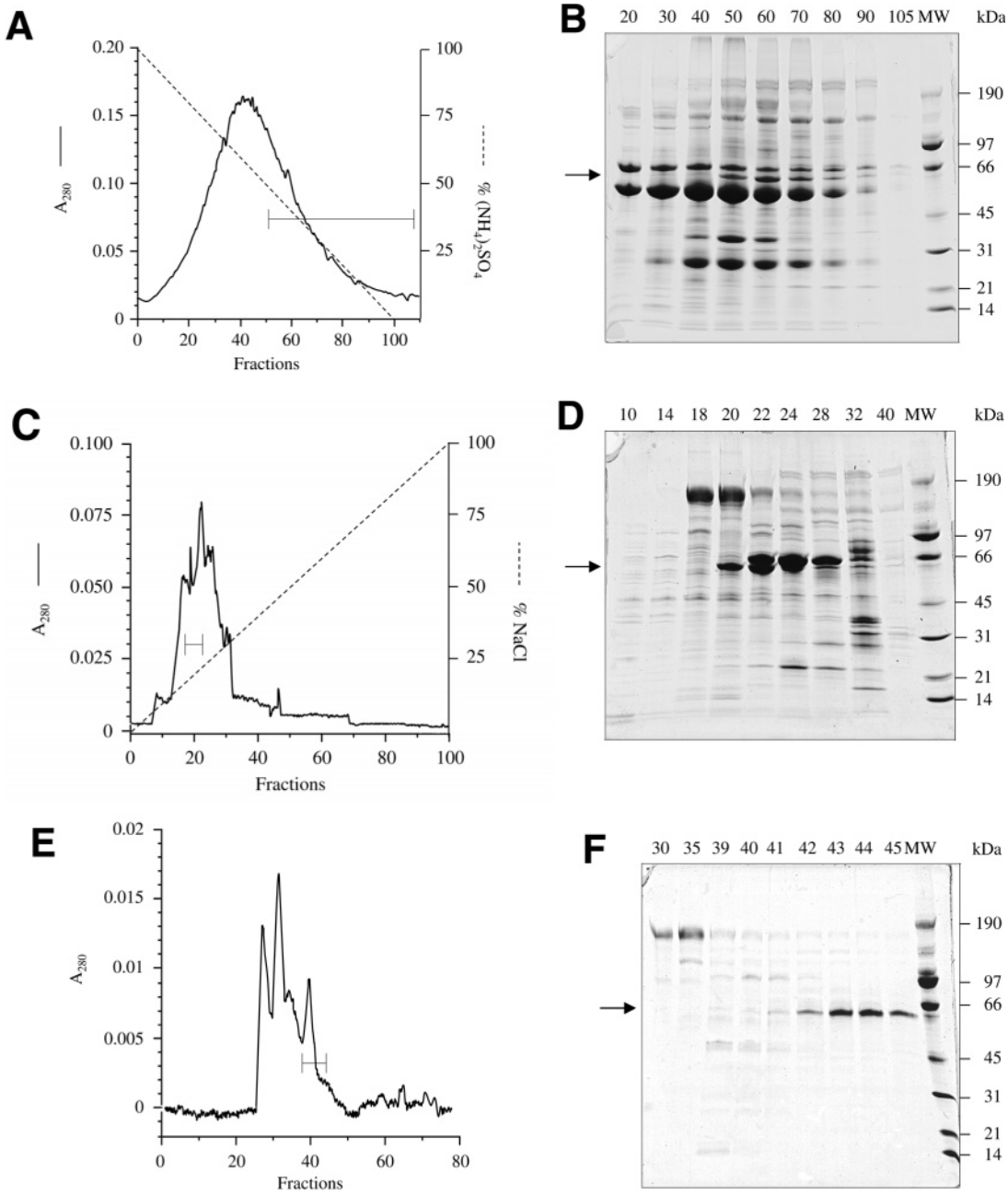

FIGURE 1: Purification of porcine corneal TGFBIp. Chromatography traces and polyacrylamide gels from purification of porcine corneal TGFBIp on Phenyl Sepharose (A, B), Mono Q (C, D), and Superose 12 (E, F). In the chromatographic traces, the bars indicate the fractions pooled for further purification. In the polyacrylamide gels, a broad set of fractions are represented, with the number of the fraction above the lane. The TGFBIp bands are indicated with arrows.

thoroughly and then frozen in liquid nitrogen. This makes them brittle, and the homogenization produces a fine powder, maximizing protein extraction. The amount of contaminating proteins in the TGFBIp extract was significantly reduced by briefly washing the pellet with water three times, which was particularly important with regard to albumin. Most of the TGFBIp could be released from the pellet by washing overnight with 1 M $(NH_4)_2SO_4$. This result suggests that the interaction with the pellet involves electrostatic interactions. The extracted proteins were applied directly to a Phenyl Sepharose column for hydrophobic interaction chromatography (Figure 1A,B). The TGFBIp-containing fractions were pooled and applied to a Protein G column to remove IgG, which was the most abundant protein in the extract. The flow-through was collected, dialyzed and applied to a Mono Q anion exchange column equilibrated in 20 mM Tris-HCl, pH 7.4 and eluted using a linear NaCl gradient (Figure 1C,D). Additional purification was achieved by gel filtration on a Superose 12 column (Figure 1E,F), yielding ~95% pure TGFBIp (Table 1). The total protein concentration was determined by absorbance at 280 nm. The progress of the purification procedure was monitored by SDS−PAGE and Western blotting. Quantification of the latter is the basis of the estimated purification folds in Table 1. Human TGFBIp was purified essentially as described above, but at a much smaller scale employing only 10 corneas (data not shown).

C-Terminal Truncation of TGFBIp. Porcine corneal TGFBIp migrates as a 64 kDa protein (Figure 1), and human corneal TGFBIp migrates as a 65 kDa protein in reduced SDS−PAGE (Figure 5A), whereas the sequence of the

Table 1: Purification Yields of Porcine Corneal TGFBIp[a]

fraction	volume (mL)	total protein (mg)	TGFBIp (mg)	yield (%)	purification (fold)
Corneal extract	300	480	1.1	100	1
Phenyl sepharose	240	96	1.0	91	4.5
Protein G column	260	39	0.9	82	10
Mono Q ion exchange	10	1.6	0.2	18	55
Superose 12 gel filtration	3	0.1	0.1	9	440

[a] The total amounts of protein are calculated from A_{280}, while the amounts of TGFBIp are estimated from quantifications using Western blotting.

TGFBI gene predicts a molecular mass of 72 kDa when excluding the signal peptide of 23 amino acid residues. We hypothesized that the smaller than expected size was the result of proteolytic processing. Thus, using Edman degradation, we identified the first eight amino acids of purified porcine TGFBIp as GPAKSPYQ (data not shown). This was the expected N-terminal sequence (*46*) and N-terminal processing was ruled out as the reason for the apparent low molecular weight. Since the N-terminal was intact, a C-terminal truncation was investigated. To identify the C-terminus, we subjected purified porcine TGFBIp to C-terminal protein sequence analysis and identified DELA-COOH as the major C-terminus and LEVSSK-COOH as a weak C-terminal sequence according to the signal intensities from the sequence HPLC (data not shown). In porcine TGFBIp, these sequences are unique to $Asp_{644}-Ala_{647}$ and $Leu_{597}-Lys_{602}$, respectively (Figure 2). To further investigate the C-terminal truncation, TGFBIp from human and porcine corneas was analyzed by LC-MS/MS. Corneal powders from porcine and human were boiled in reducing SDS sample buffer and analyzed by SDS−PAGE. The TGFBIp band was excised and digested with different proteases to generate overlaps and thereby covering most of the sequence (Table 2). This direct procedure facilitates that no proteolytic cleavages of TGFBIp occur prior to the LC-MS/MS analysis. The predominant C-terminal processing of porcine TGFBIp at Ala_{647} was verified by the presence of the truncated peptide TINTVLRPPANKPQERGDELA after digestion with chymotrypsin that does not readily cleave Ala−Xxx peptide bonds. The most C-terminal localized peptide $Gly_{643}-Lys_{655}$ was identified by LC-MS/MS of porcine TGFBIp after digestion with trypsin indicating that the C-terminal processing of TGFBIp is a heterogeneous event in the cornea. Similarly, the most C-terminal localized peptide identified in human TGFBIp was $Leu_{646}-Ala_{657}$ after digestion with thermolysin, which does not readily cleave Ala−Ser peptide bonds (Table 2, Figure 3). Thus, the LC-MS/MS analysis supports the C-terminal sequencing data using purified TGFBIp and indicates that the C-terminal of porcine corneal TGFBIp is ragged.

The predicted molecular mass of porcine TGFBIp with a C-terminus at Ala_{647} and no posttranslational modifications is 68.092 Da, and using purified TGFBIp we determined it to be 68.079 Da by MALDI mass spectrometry under nonreducing conditions (Figure 4A). To investigate the C-terminal proteolytic processing in vitro, recombinant human TGFBIp was expressed in HEK293 cells and purified from the medium. The measured mass of recombinant TGFBIp was 69.193 Da (data not shown), which is in agreement with the calculated mass (68.230 Da) following a C-terminal cut at Ala_{647}. Thus, these results suggest that the C-terminal proteolytic processing of TGFBIp in the cornea is similar to that observed when the protein is expressed in HEK293 cells.

No Evidence for Posttranslational Additions in TGFBIp. In addition to the measured masses of porcine and human TGFBIp the measured masses of the individual peptides identified by LC-MS/MS were consistent with the lack of posttranslational additions (Table 2). The only exceptions were oxidations or deamidations, which are commonly observed nonenzymatic modifications often caused by handling during protein and peptide purifications. However, since some regions of both porcine and human TGFBIp were not covered by the LC-MS/MS analysis (Table 2), we cannot exclude that TGFBIp contains posttranslational additions. Furthermore, modified peptides present in very low amounts relative to the nonmodified species could theoretically remain undetected by LC-MS/MS. However, the LC-MS/MS data revealed no evidence for posttranslational additions in TGFBIP, which is in accordance with the MALDI mass spectrometry data of both porcine and human TGFBIp.

TGFBIp Is a Monomer. During gel filtration, porcine TGFBIp eluted at a position that corresponded to an apparent molecular mass of 64.6 kDa calculated from equation: $K_{av} = 0.872 - 0.338 \times \log(MW)$ (Figure 4B), or a Stokes radius of 35.6 Å. For human corneal TGFBIp, a similar result was obtained (data not shown). In addition, cross-linking with the homobifunctional reagent dimethyl suberimidate did not result in the appearance of dimeric or other oligomeric species when analyzed by SDS−PAGE (data not shown). Thus, these results in combination with the determined molecular mass of porcine TGFBIp (68.079 Da) and rh-TGFBIp (69.193) by MALDI mass spectrometry under nonreducing conditions suggest that TGFBIp is a globular monomer.

Intact TGFBIp Is Present in Corneal Extracts. To investigate the nature of the proteolytical processing, we raised an antibody against a synthetic peptide corresponding to the entire missing C-terminus ($Asp_{648}-His_{683}$) of the predominant processed isoform of porcine TGFBIp, i.e., $Gly_{24}-Ala_{647}$. This antibody did not exhibit an affinity for purified porcine or semi-purified human TGFBIp (data not shown), indicating that the majority of human corneal TGFBIp is also lacking residues $Asp_{648}-His_{683}$. However, in Western blots of extracts from human or porcine corneas, the C-terminal antibody showed reactivity against two bands that migrated just above purified TGFBIp (Figure 5B). The faint upper band and the lower stronger band (Figure 5B) must likely represent full-length TGFBIp and the $Gly_{24}-Ala_{657}$ isoform, respectively. The reactivity was much less than with the antibody directed against the central FAS domains ($Gly_{134}-Pro_{500}$) (Figure 5A), indicating that full-length TGFBIp is significantly less abundant in the cornea than C-terminal-processed TGFBIp. To confirm the presence of full-length

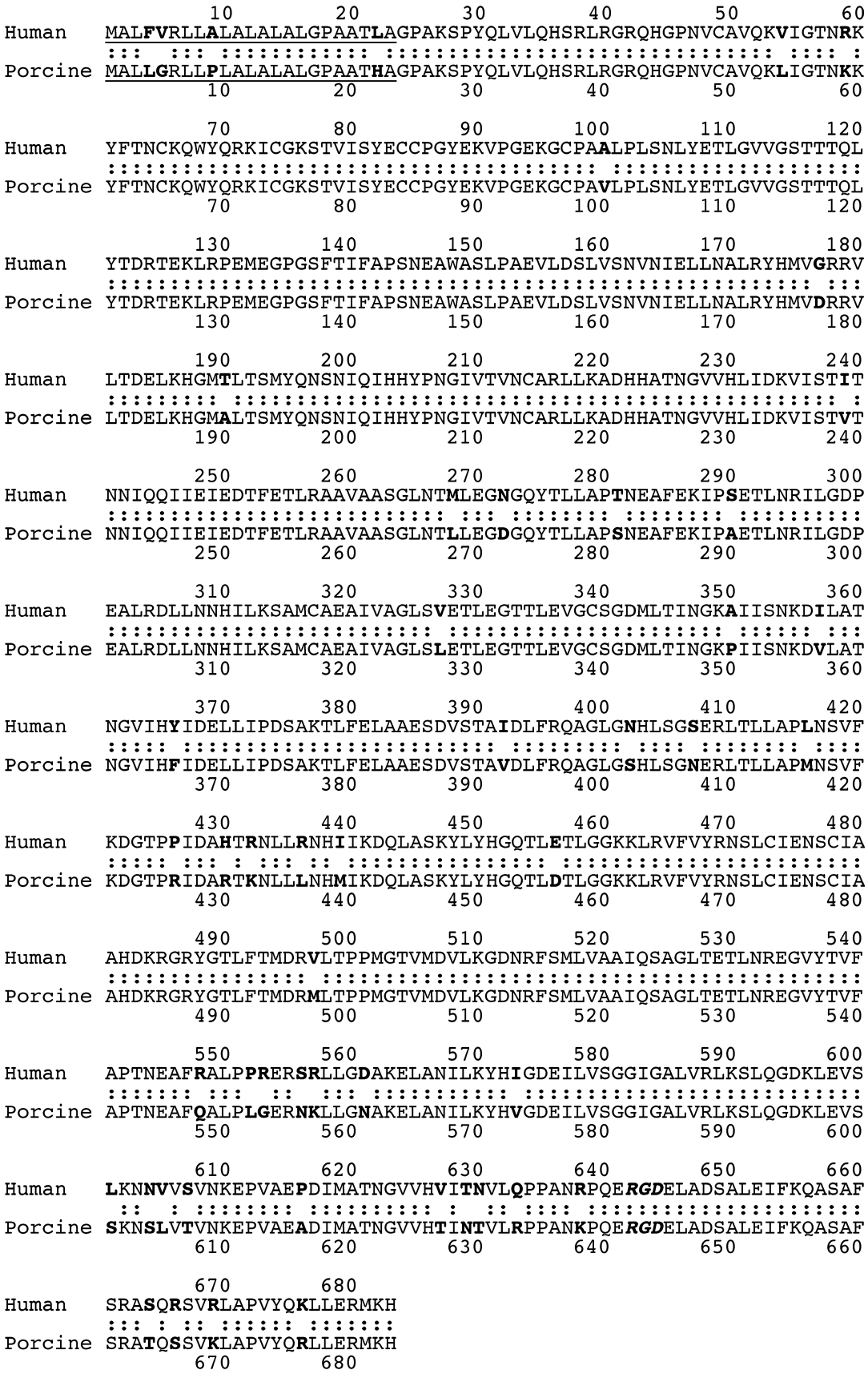

FIGURE 2: Alignment of human and porcine TGFBIp. Full-length human and porcine TGFBIp (683 residues) including the signal peptide (underlined) are 93% identical. The alignment indicates identities (regular letters) and nonidentical residues (regular bold letters). The proposed integrin binding sequence $Arg_{642}-Gly_{643}-Asp_{644}$ (RGD) is also marked (bold italic letters).

TGFBIp indicated by the Western blots, we cut out the corresponding region from a duplicate SDS−PAGE gel of extract from porcine corneas. The protein in the gel plug was digested with trypsin and the resulting peptides were

Table 2: LC-MS/MS Analyses of Porcine and Human TGFBIp[a]

residue	sequence (porcine TGFBIp)	enzyme
24−31	GPAKSPYQ	thermolysin
32−39	LVLQHSRL	thermolysin
40	R	missing
41−52	GRQHGPNVCAVQ	chymotrypsin
43−53	QHGPNVCAVQK	trypsin
54	L	missing
55−62	IGTNKKYF	chymotrypsin
62−68	FTNCKQW	thermolysin
69−72	YQRK	missing
73−82	ICGKSTVISY	chymotrypsin
79−99	VISYECCPGYEKVPGEKGCPA	thermolysin
100−103	VLPL	missing
104−121	SNLYETLGVVGSTTTQLY	chymotrypsin
122−127	TDRTEK	missing
128−140	LRPEMEGPGSFTI	thermolysin
140−158	FAPSNEAWAS LPAEVLDS	thermolysin
159−170	LVSNVNIELLNA	thermolysin
171−172	LR	missing
173−178	YHMVDR	trypsin
179	R	missing
180−186	VLTDELK	trypsin
187−213	HGMALTSMYQNSNIQIHHYPNGI VTVN	trypsin
214−219	CARLLK	missing
220−234	ADHHATNGVVHLIDK	trypsin
235−257	VISTVTNNIQQIIEIEDTFETLR	trypsin
257−275	RAAVAASGLNTLLEGDGQY	chymotrypsin
276−283	TLLAPSNE	missing
284−292	AFEKIPAETL	thermolysin
288−295	IPAETLNR	trypsin
296−304	ILGDP EALR	trypsin
305−313	DLLNNHILK	trypsin
313−325	KSAMCAEAIVAGL	chymotrypsin
326−329	SLET	missing
330−343	LEGTTLEVGCSGDM	thermolysin
344−350	LTINGKP	missing
351−366	IISNKDVLATNGVIHF	thermolysin
367−380	IDELLIPDSAKTLF	chymotrypsin
378−396	TLFELAAESDVSTAVDLFR	chymotrypsin
397−409	QAGLGSHLSGNER	trypsin
410−421	LTLLAPMNSVFK	trypsin
419−426	VFKDGTPR	thermolysin
427−432	IDARTK	missing
433−441	NLLLNHMIK	trypsin
437−448	NHMIKDQLASKY	chymotrypsin
448−461	YLYHGQTLDTLGGK	trypsin
462−464	KLR	missing
465−475	VFVYRNSLCIE	V8
473−488	CIENSCIAAHDKRGRY	chymotrypsin
488−496	YGTLFTMDR	trypsin
497−510	MLTPPMGTVMDVLK	trypsin
498−514	LTP PMGTVMDVLKGDNR	thermolysin
515−533	FSMLVAAIQSAGLTETLNR	trypsin
534−555	EGVYTVFAPTNEAFQALPLGER	trypsin
546−564	AFQALPLGERNKLLGNAKE	V8
564−570	ELANILK	trypsin
571−588	YHVGDEILVSGGIGALVR	trypsin
589−590	LK	missing
591−602	SLQGDKLEVSSK	trypsin
603−642	NSLVTVNKEPVAEADIMATNGVV HTINTVLRPPANKPQER	trypsin
627−647	TINTVLRPPANKPQERGDELA	chymotrypsin
643−655	GDELADSALEIFK	trypsin

residue	sequence (human TGFBIp)	enzyme
24−31	GPAKSPYQ	thermolysin
31−39	QLVLQHSRL	chymotrypsin
40	R	missing
41−61	GRQHGPNVCAVQKVIGTNRKY	chymotrypsin
60−66	KYFTNCK	trypsin
67−69	QWY	missing
70−82	QRKICGKSTVISY	chymotrypsin
83−95	ECCPGYEKVPGEK	chymotrypsin
96−124	GCPAALPLSNLYETLGVVGSTTTQLYTDR	trypsin
121−139	YTDRTEKLRPEMEGPGSFT	thermolysin

Table 2: Continued

residue	sequence (human TGFBIp)	enzyme
140−146	IFAPSNE	missing
147−158	AWASLPAEVLDS	thermolysin
157−168	DSLVSNVNIELL	chymotrypsin
169−172	NALR	missing
173−178	YHMVGR	trypsin
179−186	RVLTDELK	trypsin
182−191	TDELKHGMTL	chymotrypsin
192−195	TSMY	missing
196−203	QNSNIQIH	chymotrypsin
201−208	QIHHYPNG	thermolysin
209−217	IVTVNCARL	missing
218−230	LKADHHATNGVVH	thermolysin
220−234	ADHHATNGVVHLIDK	trypsin
235−257	VISTITNNIQQIIEIEDTFETLR	trypsin
258−287	AAVAASGLNTMLEGNGQYTLLAPTNEAFEK	trypsin
288−295	IPSETLNR	trypsin
296−304	ILGDPEALR	trypsin
305−313	DLLNNHILK	trypsin
314−330	SAMCAEAIVAGLSVETL	missing
331−343	EGTTLEVGCSGDM	thermolysin
344−349	LTINGK	missing
350−355	AIISNK	trypsin
356−377	DILATNGVIHYIDELLIPDSAK	trypsin
378−396	TLFELAAESDVSTAIDLFR	trypsin
397−409	QAGLGNHLSGNER	trypsin
410−421	LTLLAPLNSVFK	trypsin
421−435	KDGTPPIDAHTRNLL	chymotrypsin
436−448	RNHIIKDQLASKY	chymotrypsin
448−461	YLYHGQTLDTLGGK	trypsin
462	K	missing
463−466	LRVF	thermolysin
467−469	VYR	missing
470−485	NSLCIENSCIAAHDKR	trypsin
473−488	CIENSCIAAHDKRGRY	chymotrypsin
488−496	YGTLFTMDR	trypsin
493−506	TMDRVLTPPMGTVM	chymotrypsin
507−518	DVLKGDNRFSML	chymotrypsin
515−533	FSMLVAAIQSAGLTETLNR	trypsin
534−548	EGVYTVFAPTNEAFR	trypsin
547−555	FRALPPRER	thermolysin
556−569	SRLLGDAKELANIL	chymotrypsin
570−586	KYHIGDEILVSGGIGAL	chymotrypsin
587−601	VRLKSLQGDKLEVSL	chymotrypsin
602−619	KNNVVSVNKEPVAEPDIM	chymotrypsin
611−642	EPVAEPDIMATNGVVHVITNVLQPPANRPQER	trypsin
643−655	GDELADSALEIFK	trypsin
646−657	LADSALEIFKQA	thermolysin

[a] Top table, TGFBIp from porcine. Bottom table, TGFBIp from human. The sequence of TGFBIp is shown starting at the top of and going down the columns with overlaps where there is a change of protease. The tables show only nonredundant peptides, i.e., a peptide is only shown if at least part of the sequence is not covered by another already listed peptide.

analyzed using MALDI-TOF MS. Among the fragments identified was the peptide LAPVYQR (Leu_{670}−Arg_{676}) of TGFBIp. This is the most C-terminal peptide that we could expect to detect with the method applied (Figure 2). This demonstrates that both intact and C-terminally truncated TGFBIp are present in the cornea.

A Fraction of TGFBIp Is Covalently Associated with Insoluble ECM Components. The insoluble pellets from the human and porcine TGFBIp purifications contained TGFBIp. To investigate the nature of the binding, homogenized human and porcine corneas were washed and boiled several times in nonreducing SDS sample buffer until no TGFBIp was released. Addition of the reducing agent, DTT, to this extensively washed pellet released a significant amount of TGFBIp (Figure 6). The relative amount of covalent-associated TGFBIp was quantified by densitometry using immunoblotting, and it was estimated that approximately 60% of the total TGFBIp in the cornea was covalently associated with insoluble ECM components through a disulfide bridge. In addition, fractions of both the free and the covalently bound TGFBIp were fragmented. Fragments of TGFBIp have previously been observed in normal human corneas (*47*). Significantly, no difference in fragmentation pattern was observed between the free and the covalently bound TGFBIp.

DISCUSSION

Several corneal dystrophies are linked to mutations in the *TGFBI* gene leading to abnormal accumulations of TGFBIp aggregates in the corneal stroma and visual impairment. In this study, we purified and characterized TGFBIp from normal porcine and human corneas to obtain a better understanding of the structure and processing of this protein.

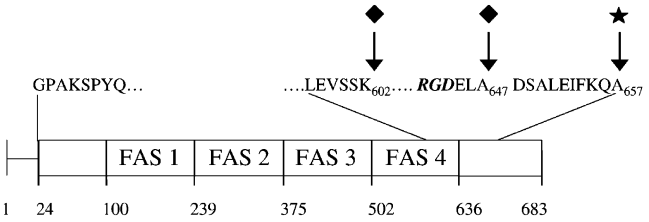

FIGURE 3: Schematic presentation of the identified TGFBIp isoforms. The scheme shows the C-terminal cleavage sites (arrows) identified in corneal porcine (◆) and human (★) TGFBIp. The RGD sequence (Arg_{642}−Asp_{644}) is only three residues from the C-terminal residue in the major isoform of mature TGFBIp (Gly_{24}−Ala_{647}) from porcine corneas. The signal peptide (Met_1−Ala_{23}) is cleaved off before TGFBIp is secreted. The four repeat Fas1 domains (Ala_{100}−Ile_{238}, Thr_{239}−Asp_{374}, Ser_{375}−Pro_{501}, and Met_{502}−Pro_{635}) are indicated.

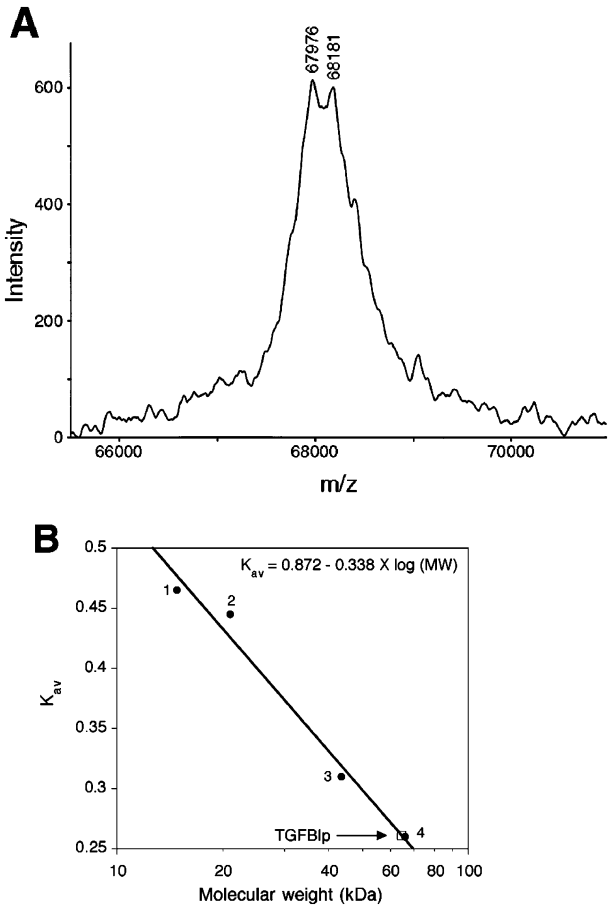

FIGURE 4: TGFBIp is a monomer. Determination of the molecular mass of purified porcine TGFBIp using MALDI mass spectrometry under nonreducing conditions (A). Determination of the apparent molecular weight of TGFBIp using calibrated gel filtration (B). The elution volumes (V_e) of the standard proteins were as follows: (1) ribonuclease A (V_e = 1.57 mL), (2) chymotrypsinogen A (V_e = 1.54 mL), (3) ovalbumin (V_e = 1.33 mL), and (4) bovine serum albumin (V_e = 1.26 mL). The elution volume of purified porcine TGFBIp (V_e = 1.256 mL) is indicated with an arrow.

The results show that the majority of corneal TGFBIp from both porcine and human are C-terminal proteolytically processed between Lys_{602} and Ser_{658}. We identified two C-termini of porcine corneal TGFBIp (Ala_{647} and Lys_{602}) and one of human corneal TGFBIp (Ala_{657}). Thus, we conclude that the C-terminal of TGFBIp is ragged in porcine corneas and that human corneas contain at least one C-terminal truncated isoform. According to the relative signal intensities

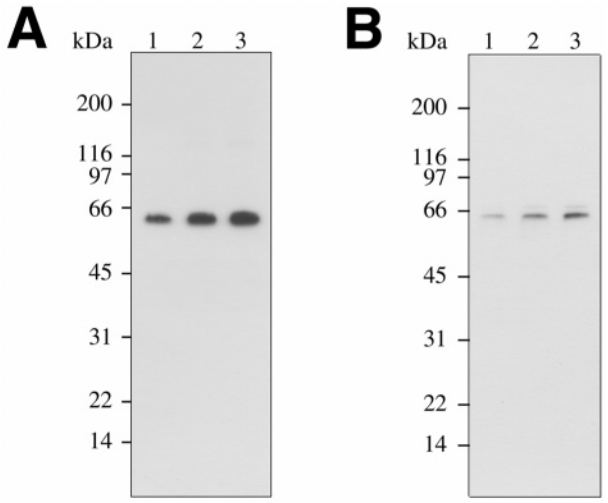

FIGURE 5: The human cornea contains both intact and C-terminally truncated TGFBIp. Normal human corneal extract was analyzed by Western blotting using antibodies against the central domains (A) and the C-terminal fragment (B). Approximately 0.1 mg was boiled in 100 μL of loading buffer containing DTT and 0.1, 0.2, or 0.3 μL of supernatant was loaded in lanes 1, 2, 3 (A), and 1, 2, and 3 μL was loaded in the gel used for the C-terminal antiserum (B).

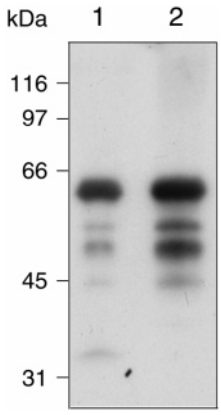

FIGURE 6: TGFBIp is covalently associated with insoluble components of the extracellular matrix. Western blot of nonreducing and reducing extractions of the human corneal powder. Lane 1, supernatant following extraction using nonreducing SDS sample buffer; lane 2, supernatant following extraction using SDS sample buffer containing DTT. Both lanes contain 1/10 of the extract from 1 mg of corneal powder. It is apparent that a significant amount (~60% as determined by densitometry) of TGFBIp is released from the pellet following the addition of DTT. In addition, some TGFBIp was fragmented in agreement with previous reports (*47*).

from the C-terminal sequencing analysis, the most abundant isoform of TGFBIp in porcine corneas is truncated at Ala_{647} leaving only three amino acids between the integrin binding RGD sequence and the mature C-terminal residue. Because secondary structure predictions show that the RGD sequence is part of an α-helix in full-length TGFBIp, but forms a random coil after processing of the Ala_{647}−Asp_{648} peptide bond, the processing may represent a functional activation of the integrin binding activity. In this scenario, the processing would make the area around the RGD sequence more accessible and thereby facilitate the binding to integrins. Unmasking of hidden or so-called cryptic sequences is an important mode of regulation in the extracellular matrix (*48*). In addition, we identified a mature C-terminus at Lys_{602} in porcine corneal TGFBIp. This finding may indicate the

release of a C-terminal TGFBIp peptide containing the RGD following proteolytic processing. Previous results have indicated that the release of a C-terminal TGFBIp peptide containing the RGD sequence mediates apoptosis (*49*). The C-terminal processing of porcine and human corneal TGFBIp was verified by immunoblotting using antibodies raised against the *central* and C-*terminal* regions of TGFBIp. The results showed that isoforms lacking the C-terminal region were much more abundant than the full-length isoform in extracts of human and porcine corneas. In addition, the measured mass of human recombinant TGFBIp expressed in HEK293 cells indicates that the proteolytic processing in vitro is similar to that in vivo. All the residues mutated in TGFBIp-linked corneal dystrophies are maintained in the major isoform of C-terminal truncated porcine TGFBIp (residues Gly_{24}−Ala_{647}) and human TGFBIp (residues Gly_{24}−Ala_{657}). In contrast, the residues Ala_{622}, Gly_{623}, and His_{626} are not preserved in the porcine TGFBIp isoform cleaved at Lys_{602}.

Many FAS proteins including periostin, the closest homologue of TGFBIp, are glycosylated, and it has previously been reported that TGFBIp is phosphorylated (*50*). However, the data presented here reveal no evidence that TGFBIp carries posttranslational additions. This conclusion rests on two findings: (a) the determined mass of TGFBIp corresponds to the theoretical mass of the unmodified protein and (b) an extensive search for modified peptides using LC-MS/MS was unsuccessful.

The retention of TGFBIp in gel filtration indicates that the native protein is a monomer with a globular shape. This finding is in contrast to observations of multimerization by Kim et al. (*51*) and Ohno et al. (*20*). We did not encounter natural multimers of TGFBIp, but after denaturation prior to nonreduced SDS−PAGE, TGFBIp was prone to disulfide bridge exchange and dimerization. This could be completely eliminated by carboxymethylation of free Cys residues before denaturation. In addition, dimers were not observed in gel filtration chromatography or native PAGE, presumably because the native state protects TGFBIp against disulfide-bridge exchange.

TGFBIp has recently been shown to bind bovine collagen VI through a disulfide bond in tissue microfibrils (*27*). Our observation that a large fraction of human TGFBIp can be released from the cornea pellet by reduction shows that the same binding is likely to exist in the human cornea. This is particularly likely as the cornea has an exceptionally high content of collagen VI, estimated up to 25% of the total protein (*52*). The covalently bound fraction of TGFBIp was not analyzed by mass spectrometry and, therefore, it may have different structural characteristics than the soluble fraction of TGFBIp.

In conclusion, we have purified TGFBIp from porcine and human corneas. The proteins were shown to be a monomer in both cases. In addition the C-terminals were truncated predominantly just after the RGD sequence. TGFBIp presumably does not carry posttranslational additions, but approximately 60% of the protein is covalently associated with insoluble components of the extracellular matrix.

ACKNOWLEDGMENT

We thank Dr. Steen Vang Petersen for helpful discussions and assistance in the production of antibodies.

REFERENCES

1. Skonier, J., Neubauer, M., Madisen, L., Bennett, K., Plowman, G. D., and Purchio, A. F. (1992) cDNA cloning and sequence analysis of beta ig-h3, a novel gene induced in a human adenocarcinoma cell line after treatment with transforming growth factor-beta, *DNA Cell Biol. 11*, 511−522.
2. Hirate, Y., Tomita, K., Yamamoto, S., Kobari, K., Uemura, I., Yamasu, K., and Suyemitsu, T. (1999) Association of the sea urchin EGF-related peptide, EGIP-D, with fasciclin I-related ECM proteins from the sea urchin Anthocidaris crassispina, *Dev., Growth Differ. 41*, 483−494.
3. Huber, O., and Sumper, M. (1994) Algal-CAMs: isoforms of a cell adhesion molecule in embryos of the alga Volvox with homology to Drosophila fasciclin I, *EMBO J. 13*, 4212−4222.
4. Shi, H., Kim, Y., Guo, Y., Stevenson, B., and Zhu, J. K. (2003) The Arabidopsis SOS5 Locus Encodes a Putative Cell Surface Adhesion Protein and Is Required for Normal Cell Expansion, *Plant Cell 15*, 19−32.
5. Matsumoto, S., Matsuo, T., Ohara, N., Hotokezaka, H., Naito, M., Minami, J., and Yamada, T. (1995) Cloning and sequencing of a unique antigen MPT70 from *Mycobacterium tuberculosis* H37Rv and expression in BCG using E. coli-mycobacteria shuttle vector, *Scand. J. Immunol. 41*, 281−287.
6. Zinn, K., McAllister, L., and Goodman, C. S. (1988) Sequence analysis and neuronal expression of fasciclin I in grasshopper and Drosophila, *Cell 53*, 577−587.
7. Carr, M. D., Bloemink, M. J., Dentten, E., Whelan, A. O., Gordon, S. V., Kelly, G., Frenkiel, T. A., Hewinson, R. G., and Williamson, R. A. (2003) Solution structure of the *Mycobacterium tuberculosis* complex protein MPB70: from tuberculosis pathogenesis to inherited human corneal disease, *J. Biol. Chem. 278*, 43736−43743.
8. Takeshita, S., Kikuno, R., Tezuka, K., and Amann, E. (1993) Osteoblast-specific factor 2: cloning of a putative bone adhesion protein with homology with the insect protein fasciclin I, *Biochem. J. 294*, 271−278.
9. Horiuchi, K., Amizuka, N., Takeshita, S., Takamatsu, H., Katsuura, M., Ozawa, H., Toyama, Y., Bonewald, L. F., and Kudo, A. (1999) Identification and characterization of a novel protein, periostin, with restricted expression to periosteum and periodontal ligament and increased expression by transforming growth factor beta, *J. Bone Miner. Res. 14*, 1239−1249.
10. Adachi, H., and Tsujimoto, M. (2002) FEEL-1, a novel scavenger receptor with in vitro bacteria-binding and angiogenesis-modulating activities, *J. Biol. Chem. 277*, 34264−34270.
11. Tamura, Y., Adachi, H., Osuga, J., Ohashi, K., Yahagi, N., Sekiya, M., Okazaki, H., Tomita, S., Iizuka, Y., Shimano, H., Nagai, R., Kimura, S., Tsujimoto, M., and Ishibashi, S. (2003) FEEL-1 and FEEL-2 are endocytic receptors for advanced glycation end products, *J. Biol. Chem. 278*, 12613−12617.
12. Politz, O., Gratchev, A., McCourt, P. A., Schledzewski, K., Guillot, P., Johansson, S., Svineng, G., Franke, P., Kannicht, C., Kzhyshkowska, J., Longati, P., Velten, F. W., and Goerdt, S. (2002) Stabilin-1 and -2 constitute a novel family of fasciclin-like hyaluronan receptor homologues, *Biochem. J. 362*, 155−164.
13. Hu, S., Sonnenfeld, M., Stahl, S., and Crews, S. T. (1998) Midline Fasciclin: a Drosophila Fasciclin-I-related membrane protein localized to the CNS midline cells and trachea, *J. Neurobiol. 35*, 77−93.
14. Clout, N. J., Tisi, D., and Hohenester, E. (2003) Novel Fold Revealed by the Structure of a FAS1 Domain Pair from the Insect Cell Adhesion Molecule Fasciclin I, *Structure (Camb) 11*, 197−203.
15. Clout, N. J., and Hohenester, E. (2003) A model of FAS1 domain 4 of the corneal protein betaig-h3 gives a clearer view on corneal dystrophies, *Mol. Vis. 9*, 440−448.
16. Escribano, J., Hernando, N., Ghosh, S., Crabb, J., and Coca-Prados, M. (1994) cDNA from human ocular ciliary epithelium homologous to beta ig-h3 is preferentially expressed as an extracellular protein in the corneal epithelium, *J. Cell. Physiol. 160*, 511−521.
17. Rawe, I. M., Zhan, Q., Burrows, R., Bennett, K., and Cintron, C. (1997) Beta-ig. Molecular cloning and in situ hybridization in corneal tissues, *Invest. Ophthalmol. Vision Sci. 38*, 893−900.
18. LeBaron, R. G., Bezverkov, K. I., Zimber, M. P., Pavelec, R., Skonier, J., and Purchio, A. F. (1995) Beta IG-H3, a novel secretory protein inducible by transforming growth factor-beta,

is present in normal skin and promotes the adhesion and spreading of dermal fibroblasts in vitro, *J. Invest. Dermatol. 104*, 844−849.
19. Kitahama, S., Gibson, M. A., Hatzinikolas, G., Hay, S., Kuliwaba, J. L., Evdokiou, A., Atkins, G. J., and Findlay, D. M. (2000) Expression of fibrillins and other microfibril-associated proteins in human bone and osteoblast-like cells, *Bone 27*, 61−67.
20. Ohno, S., Doi, T., Fujimoto, K., Ijuin, C., Tanaka, N., Tanimoto, K., Honda, K., Nakahara, M., Kato, Y., and Tanne, K. (2002) RGD-CAP (betaig-h3) exerts a negative regulatory function on mineralization in the human periodontal ligament, *J. Dent. Res. 81*, 822−825.
21. Ferguson, J. W., Thoma, B. S., Mikesh, M. F., Kramer, R. H., Bennett, K. L., Purchio, A., Bellard, B. J., and LeBaron, R. G. (2003) The extracellular matrix protein betaIG-H3 is expressed at myotendinous junctions and supports muscle cell adhesion, *Cell Tissue Res. 313*, 93−105.
22. Carson, D. D., Lagow, E., Thathiah, A., Al-Shami, R., Farach-Carson, M. C., Vernon, M., Yuan, L., Fritz, M. A., and Lessey, B. (2002) Changes in gene expression during the early to mid-luteal (receptive phase) transition in human endometrium detected by high-density microarray screening, *Mol. Hum. Reprod. 8*, 871−879.
23. Lee, S. H., Bae, J. S., Park, S. H., Lee, B. H., Park, R. W., Choi, J. Y., Park, J. Y., Ha, S. W., Kim, Y. L., Kwon, T. H., and Kim, I. S. (2003) Expression of TGF-beta-induced matrix protein betaig-h3 is up-regulated in the diabetic rat kidney and human proximal tubular epithelial cells treated with high glucose, *Kidney Int. 64*, 1012−1021.
24. Schorderet, D. F., Menasche, M., Morand, S., Bonnel, S., Buchillier, V., Marchant, D., Auderset, K., Bonny, C., Abitbol, M., and Munier, F. L. (2000) Genomic characterization and embryonic expression of the mouse Bigh3 (Tgfbi) gene, *Biochem. Biophys. Res. Commun. 274*, 267−274.
25. Ferguson, J. W., Mikesh, M. F., Wheeler, E. F., and LeBaron, R. G. (2003) Developmental expression patterns of Beta-ig (betaIG-H3) and its function as a cell adhesion protein, *Mech. Dev. 120*, 851−864.
26. Gibson, M. A., Kumaratilake, J. S., and Cleary, E. G. (1997) Immunohistochemical and ultrastructural localization of MP78/70 (betaig-h3) in extracellular matrix of developing and mature bovine tissues, *J. Histochem. Cytochem. 45*, 1683−1696.
27. Hanssen, E., Reinboth, B., and Gibson, M. A. (2003) Covalent and noncovalent interactions of betaig-h3 with collagen VI. Beta ig-h3 is covalently attached to the amino-terminal region of collagen VI in tissue microfibrils, *J. Biol. Chem. 278*, 24334−24341.
28. Hashimoto, K., Noshiro, M., Ohno, S., Kawamoto, T., Satakeda, H., Akagawa, Y., Nakashima, K., Okimura, A., Ishida, H., Okamoto, T., Pan, H., Shen, M., Yan, W., and Kato, Y. (1997) Characterization of a cartilage-derived 66-kDa protein (RGD-CAP/beta ig-h3) that binds to collagen, *Biochim. Biophys. Acta 1355*, 303−314.
29. Billings, P. C., Whitbeck, J. C., Adams, C. S., Abrams, W. R., Cohen, A. J., Engelsberg, B. N., Howard, P. S., and Rosenbloom, J. (2002) The transforming growth factor-beta-inducible matrix protein (beta)ig-h3 interacts with fibronectin, *J. Biol. Chem. 277*, 28003−28009.
30. Kim, J. E., Kim, S. J., Lee, B. H., Park, R. W., Kim, K. S., and Kim, I. S. (2000) Identification of motifs for cell adhesion within the repeated domains of transforming growth factor-beta-induced gene, betaig-h3, *J. Biol. Chem. 275*, 30907−30915.
31. Bae, J. S., Lee, S. H., Kim, J. E., Choi, J. Y., Park, R. W., Yong Park, J., Park, H. S., Sohn, Y. S., Lee, D. S., Bae Lee, E., and Kim, I. S. (2002) Betaig-h3 supports keratinocyte adhesion, migration, and proliferation through alpha3beta1 integrin, *Biochem. Biophys. Res. Commun. 294*, 940−948.
32. Ohno, S., Noshiro, M., Makihira, S., Kawamoto, T., Shen, M., Yan, W., Kawashima-Ohya, Y., Fujimoto, K., Tanne, K., and Kato, Y. (1999) RGD-CAP ((beta)ig-h3) enhances the spreading of chondrocytes and fibroblasts via integrin alpha(1)beta(1), *Biochim. Biophys. Acta 1451*, 196−205.
33. Kim, J. E., Jeong, H. W., Nam, J. O., Lee, B. H., Choi, J. Y., Park, R. W., Park, J. Y., and Kim, I. S. (2002) Identification of motifs in the fasciclin domains of the transforming growth factor-beta-induced matrix protein betaig-h3 that interact with the alphavbeta5 integrin, *J. Biol. Chem. 277*, 46159−46165.
34. Kim, M. O., Yun, S. J., Kim, I. S., Sohn, S., and Lee, E. H. (2003) Transforming growth factor-beta-inducible gene-h3 (betaig-h3) promotes cell adhesion of human astrocytoma cells in vitro: implication of alpha6beta4 integrin, *Neurosci. Lett. 336*, 93−96.
35. Munier, F. L., Korvatska, E., Djemai, A., Le Paslier, D., Zografos, L., Pescia, G., and Schorderet, D. F. (1997) Kerato-epithelin mutations in four 5q31-linked corneal dystrophies, *Nat. Genet. 15*, 247−251.
36. Klintworth, G. K. (2003) The molecular genetics of the corneal dystrophies − current status, *Front. Biosci. 8*, D687−713.
37. Klintworth, G. K., Valnickova, Z., and Enghild, J. J. (1998) Accumulation of beta ig-h3 gene product in corneas with granular dystrophy, *Am. J. Pathol. 152*, 743−748.
38. Streeten, B. W., Qi, Y., Klintworth, G. K., Eagle, R. C., Jr., Strauss, J. A., and Bennett, K. (1999) Immunolocalization of beta ig-h3 protein in 5q31-linked corneal dystrophies and normal corneas, *Arch. Ophthalmol. 117*, 67−75.
39. Klintworth, G. K., Bao, W., and Afshari, N. A. (2004) Two Mutations in the TGFBI (BIGH3) Gene Associated with Lattice Corneal Dystrophy in an Extensively Studied Family, *Invest. Ophthalmol. Vision Sci. 45*, 1382−1388.
40. Bergman, T., Cederlund, E., and Jornvall, H. (2001) Chemical C-terminal protein sequence analysis: improved sensitivity, length of degradation, proline passage, and combination with Edman degradation, *Anal. Biochem. 290*, 74−82.
41. Perkins, D. N., Pappin, D. J., Creasy, D. M., and Cottrell, J. S. (1999) Probability-based protein identification by searching sequence databases using mass spectrometry data, *Electrophoresis 20*, 3551−3567.
42. Siegel, L. M., and Monty, K. J. (1966) Determination of molecular weights and frictional ratios of proteins in impure systems by use of gel filtration and density gradient centrifugation. Application to crude preparations of sulfite and hydroxylamine reductases, *Biochim. Biophys. Acta 112*, 346−362.
43. Wellings, D. A., and Atherton, E. (1997) Standard Fmoc protocols, *Methods Enzymol. 289*, 44−67.
44. Bury, A. F. (1981) Analysis of protein and peptide mixtures, *J. Chromatogr. 213*, 491−500.
45. Matsudaira, P. (1987) Sequence from picomole quantities of proteins electroblotted onto poly(vinylidene difluoride) membranes, *J. Biol. Chem. 262*, 10035−10038.
46. Skonier, J., Bennett, K., Rothwell, V., Kosowski, S., Plowman, G., Wallace, P., Edelhoff, S., Disteche, C., Neubauer, M., Marquardt, H., and et al. (1994) beta ig-h3: a transforming growth factor-beta-responsive gene encoding a secreted protein that inhibits cell attachment in vitro and suppresses the growth of CHO cells in nude mice, *DNA Cell Biol. 13*, 571−584.
47. Korvatska, E., Henry, H., Mashima, Y., Yamada, M., Bachmann, C., Munier, F. L., and Schorderet, D. F. (2000) Amyloid and nonamyloid forms of 5q31-linked corneal dystrophy resulting from kerato-epithelin mutations at Arg-124 are associated with abnormal turnover of the protein, *J. Biol. Chem. 275*, 11465−11469.
48. Schenk, S., and Quaranta, V. (2003) Tales from the crypt[ic] sites of the extracellular matrix, *Trends Cell Biol. 13*, 366−375.
49. Kim, J. E., Kim, S. J., Jeong, H. W., Lee, B. H., Choi, J. Y., Park, R. W., Park, J. Y., and Kim, I. S. (2003) RGD peptides released from beta ig-h3, a TGF-beta-induced cell-adhesive molecule, mediate apoptosis, *Oncogene 22*, 2045−2053.
50. Srivastava, O. P., and Srivastava, K. (1999) cAMP-dependent phosphorylation of betaig-h3 protein in human corneal endothelial cells, *Curr. Eye Res. 19*, 348−357.
51. Kim, J. E., Park, R. W., Choi, J. Y., Bae, Y. C., Kim, K. S., Joo, C. K., and Kim, I. S. (2002) Molecular properties of wild-type and mutant betaIG-H3 proteins, *Invest. Ophthalmol. Vision Sci. 43*, 656−661.
52. Zimmermann, D. R., Trueb, B., Winterhalter, K. H., Witmer, R., and Fischer, R. W. (1986) Type VI collagen is a major component of the human cornea, *FEBS Lett. 197*, 55−58.

BI048589S